HOURLY SOLAR RADIATION FORECASTING THROUGH NEURAL NETWORKS AND MODEL TREES

by

CAMERON REID HAMILTON

(Under the Direction of Walter D. Potter)

ABSTRACT

Solar radiation forecasting models were developed in order to determine the specific times during a given day that solar panels could be relied upon to produce energy sufficient to meet the demand of the energy provider, Georgia Power. These models, which consisted of multilayer perceptrons (MLP), model averaged neural networks (MANN) and alternating model trees (AMT), were constructed to forecast solar radiation an hour into the future, given 2003-2012 solar radiation data from the Griffin, Georgia weather station for training and 2013 data for testing. A literature review of the most prominent hourly solar radiation models was performed and normalized root mean square error was calculated for each. The results demonstrate that MANN and AMT models outperform or parallel the highest-performing models within the literature. MANN and AMT are thus promising forecasting models that may be further improved by forming an ensemble of these models with the top performing within the literature.

INDEX WORDS: solar radiation, time series forecasting, neural networks, model trees

HOURLY SOLAR RADIATION FORECASTING THROUGH NEURAL NETWORKS AND MODEL TREES

by

CAMERON REID HAMILTON

BA, Bates College, 2012

MA, Georgia State University, 2014

A Thesis Submitted to the Graduate Faculty of The University of Georgia in Partial Fulfillment of the Requirements for the Degree

MASTER OF SCIENCE

ATHENS, GEORGIA

2016

HOURLY SOLAR RADIATION FORECASTING THROUGH NEURAL NETWORKS AND MODEL TREES

by

CAMERON REID HAMILTON

Major Professor:	Walter D. Potter
Committee:	Khaled Rasheed
	Prashant Doshi

Electronic Version Approved:

Suzanne Barbour
Dean of the Graduate School
The University of Georgia
May 2016

ACKNOWLEDGEMENTS

I would first like to thank Georgia Power for providing me with the opportunity to immerse myself within this research. I would also like to thank Dr. Potter and the Institute for Artificial Intelligence at large for offering me a graduate research assistantship to carry out this research. Dr. Doshi and Dr. Rasheed graciously served as my thesis committee members and I am grateful for their patience as I worked to complete this project. I would like to thank Mrs. Sonya Tino for helping me ensure I completed all the requirements for conference registration and travel authorization. I would finally like to thank my friends and family who have always supported my endeavors, academic or otherwise, and who have always kept my spirits high.

TABLE OF CONTENTS

Page

LIST OF TABLES

Page

LIST OF FIGURES

Page

CHAPTER 1

HOURLY SOLAR RADIATION FORECASTING

1.1 INTRODUCTION

With the advent of efficient and affordable solar energy technology, there is an increasing demand to determine how these technologies can be managed, in order to maximize the energy harvested. One method for optimizing energy production, from the perspective of energy providers, is to predict how much energy they can expect to collect from solar panels at a given time of day. With this information, an energy provider can dynamically adjust which energy sources to draw upon to deliver energy to their customers, with the intent of minimizing the use of non-renewable energy sources as often as possible. Thus, it is not surprising that the search query, "solar radiation prediction," returns 1,200,000 results on Google Scholar[1]. With a sufficiently accurate solar radiation prediction model, energy providers can reduce their use of expensive, non-renewable energy sources, and thus reduce pollution. In contrast, a poor performing model that predicts more solar radiation than actually occurs can mislead energy providers into reducing use of other energy sources, such that the energy needs of customers are not met. A model that predicts less solar radiation than actually occurs causes energy providers to miss opportunities to reduce usage of other energy. Therefore, it is imperative to develop a solar radiation prediction model that leverages state-of-the-art algorithms in time-series forecasting in order to maximize the benefits to be gained through solar energy.

[1] No analysis was performed to determine how many of the results returned actually pertain to solar radiation prediction

The objective of the current study was to develop a model of solar radiation forecasting capable of predicting the amount of solar radiation that would make contact with the surface of the earth an hour or more into the future. This endeavor was commissioned by Georgia Power with the intent of integrating the predictive model into the control system regulating which energy sources are drawn upon to meet the demand of their customers at a given time. Southern Company, the parent company of Georgia Power, currently operates facilities capable of generating over 1,400 MW from solar energy. These facilities were constructed in accordance with Southern Company's Advanced Solar Initiative (GPASI) and Integrated Resource Plan (IRP) [1]. One of the most recent initiatives undertaken by Georgia Power has been the installation of a solar farm on the University of Georgia-Athens campus, which is capable of generating 1 MW of solar energy [2]. Georgia Power and the University of Georgia have plans to continue their partnership by constructing a 3 MW solar farm on the Tifton campus [3]. Thus, a predictive model capable of forecasting the amount of solar radiation that will occur an hour or more into the future could allow Georgia Power to reduce their usage of non-renewable energy sources when the solar energy is predicted to be sufficient at a given time, while also providing the company with returns on their investment.

Data from the Georgia Automated Environmental Monitoring Network's (GAEMN)[2] Griffin weather station from 2003-2013 were used to construct the predictive models. In order to standardize performance, all models were trained with data from 2003-2012 and tested on 2013 data. Solar radiation values ranged from 0 – 1200 W/m^2. Observations were collected at 15 minute intervals over the duration of each year for a total of 35040 observations per year. Forty-three data fields were observed, though only a subset of these fields was used for solar radiation

[2] Information about GAEMN can be accessed at http://www.georgiaweather.net/

prediction: year, day of year, time of day, air temperature (°C), humidity (%), dew point (°C), vapor pressure (kPa), barometric pressure (kPa), wind speed (m/s), solar radiation (W/m^2), total solar radiation (KJ/m^2), photosynthetically active radiation ($umole/m^2s$), and rainfall (mm). In subsequent studies, only the current solar radiation amount, SR_t and the previous n solar radiation values, SR_{t-n}, …, SR_{t-2}, SR_{t-1}, were used as input to predict solar radiation an hour into the future, SR_{t+4}.

The hourly solar radiation forecasting models are characterized in Chapters 2 and 3 as follows: Chapter 2 describes an artificial neural network model that utilized air temperature, humidity, solar radiation (SR), total solar radiation (TSR), photosynthetically active radiation (PAR) and rainfall as the input fields in order to achieve a mean square error (MSE) of 0.0042, which is equivalent to a root mean squared error of 77.77 W/m^2. In addition, several models of direct normal irradiance (DNI) were constructed, which explicitly calculate an expected amount of solar radiation through empirically derived formulas pertaining to solar radiation, including local solar time, hour angle, declination angle, solar elevation angle, air mass, and absolute air mass. These models are adapted from prominent DNI models with the solar radiation literature and include WGEN [4], Hoogenboom's model [5], Yang's model [6], Iqbal's model [7], and ESRA2 [8]-[9]. These models utilize barometric pressure, latitude, and vapor pressure, in addition to observations of aerosol optical depth, water vapor, and Angstrom's coefficient taken from AERONET (http://aeronet.gsfc.nasa.gov) at the Georgia Tech site, in order to estimate DNI. The results from this study demonstrate that the same neural network trained with air temperature, humidity, SR, and the DNI calculated from the WGEN model, was able to attain the same MSE as the model trained with air temperature, humidity, solar radiation (SR), total solar radiation (TSR), photosynthetically active radiation (PAR) and rainfall.

The neural network model described in Chapter 3 improves upon the neural network characterized in Chapter 2 through two important innovations: first, significantly more previous solar radiation values (i.e. a significantly greater lag) were used as input for training the model, while the other input fields, such as rainfall and air temperature, were discarded. Second, each neural network within the ensemble was initialized with the same architecture as the previous study (except the number of input units), but with distinct weight vectors within their hidden layers, and was trained until demonstrating a decline in performance on the test set. Once trained, the predictions of these networks on a given input were averaged together in order to calculate a final prediction for solar radiation at time $t + 1$. This model, referred to as a *model averaged neural network* (MANN) [12], attained a RMSE of 62.81 W/m2 when trained on solar radiation values with a lag of 96 (i.e. 96 previous solar radiation values collected in 15 minute intervals, totaling to 24 hours).

Furthermore, although decision tree-based models are rare within the solar radiation forecasting literature, a state-of-the-art decision tree, known as an *alternating model tree* (AMT), was also implemented in this study. AMTs are composed of two types of nodes: splitter nodes, where numeric attributes are split at the median value of the attribute, and predictor nodes, which utilize linear regression to predict the numeric output at that node [11]. In addition, an AMT is grown via forward stage-wise additive modeling, where the residual errors made by the current AMT are fitted to a base learner (e.g. a decision stump or a linear regression model), after which the fitted base learner is added into the regression predictions made by the AMT. The AMT is tuned by specifying the number of iterations to grow the tree for (i) as well as the shrinkage (λ), which dampens the predictions of each base learner within the additive model towards predicting the mean of the target series. Thus, an AMT was deemed appropriate for the domain of solar

radiation, as the replacement of constant values with linear regression models at the leaf nodes of the decision tree allow AMTs to model nonlinear curves in a piecewise fashion. The AMT model with a lag of 96 attained an RMSE of 62.7 W/m^2. These results suggests that the AMT parallels the performance of the MANN and thus warrants further investigation as a solar radiation forecasting model.

A thorough literature review of the top performing and most frequently cited solar radiation prediction models was carried out for comparison with the performance of the models developed within this study. One of the reoccurring problems within the literature on solar radiation forecasting is the lack of unity in performance metrics for comparing models. As Hoff et al. [10] note, while RMSE and mean absolute error (MAE) are calculated with the same equation across studies, their calculations as percentages are not. In order to remedy this problem, normalized root mean square error (NRMSE) is calculated for top solar radiation forecasting models with in the literature. As NRMSE is calculated as a percentage error that is relative to the minimum and maximum solar radiation values observed within the respective studies, it allows models to be compared across studies. A comparison of the NRMSE of the most influential models in the literature, with the models developed in the current study, demonstrated that the MANN and AMT models outperform or parallel the performance of the models described in the literature. These results suggest the MANN and AMT developed in the current study represent the cutting-edge of solar radiation forecasting and merit investigations on how these two models can be formed into an ensemble to leverage the strengths of both models.

1.2 REFERENCES

1. Southern Company. (2016). Renewable Resources. Retrieved April 08, 2016, from http://www.southerncompany.com/what-doing/corporate-responsibility/energy-innovation/building-renewable-resources.cshtml#solar
2. UGA Office of Sustainability. (2016). Renewable Energy. Retrieved April 08, 2016, from http://sustainability.uga.edu/what-were-doing/renewable-energy/
3. UGA Office of Sustainability. (2016). Solar power initiatives expand across campus. Retrieved April 08, 2016, from http://sustainability.uga.edu/solar-power-initiatives-expand-across-campus/
4. Richardson, C.W. & Wright, D.A. (1984). WGEN: A model for generating daily weather variables. U.S. Department of Agriculture, Agricultural Research Service, ARS-8, 83.
5. Hoogenboom, G., Jones, J. W., Wilkens, P. W., Batchelor, W. D., Bowen, W. T., Hunt, L. A., ... & White, J. W. (1994). Crop models. DSSAT version, 3(2), 95-244.
6. Yang, K., Huang, G. W., &Tamai, N. (2001). A hybrid model for estimating global solar radiation. Solar energy, 70(1), 13-22.
7. Wong, L. T., & Chow, W. K. (2001). Solar radiation model. Applied Energy, 69(3), 191-224.
8. Geiger, M., Diabaté, L., Ménard, L., & Wald, L. (2002). A web service for controlling the quality of measurements of global solar irradiation. Solar energy, 73(6), 475-480.
9. Rigollier, C., Bauer, O., & Wald, L. (2000). On the clear sky model of the ESRA—European Solar Radiation Atlas—with respect to the Heliosat method. Solar energy, 68(1), 33-48.

10. Hoff, T. E., Perez, R., Kleissl, J., Renne, D., & Stein, J. (2013). Reporting of irradiance modeling relative prediction errors. *Progress in Photovoltaics: Research and Applications*, 21(7), 1514-1519.
11. Ripley, B. (1996). *Pattern recognition and neural networks.* Cambridge University Press.
12. Frank, E., Mayo, M., & Kramer, S. (2015). Alternating Model Trees. In *Proceedings of the 30th Annual ACM Symposium on Applied Computing*, 871-878.

CHAPTER 2

HOURLY SOLAR RADIATION FORECASTING THROUGH NEURAL NETWORKS AND DIRECT NORMAL IRRADIANCE MODELS[3]

[3] Hamilton, C.R., Potter, W.D., Hoogenboom, G., McClendon, R., & W. Hobbs. 2015. *International Journal of Computer, Electrical, Automation, Control and Information Engineering*. 9(5): 970-975. Reprinted here with permission of the publisher.

2.1 ABSTRACT

A model was constructed to predict the amount of solar radiation that will make contact with the surface of the earth in a given location an hour into the future. This project was supported by the Southern Company to determine at what specific times during a given day of the year solar panels could be relied upon to produce energy in sufficient quantities. Due to their ability as universal function approximators, an artificial neural network was used to estimate the nonlinear pattern of solar radiation, which utilized measurements of weather conditions collected at the Griffin, Georgia weather station as inputs. A number of network configurations and training strategies were utilized, though a multilayer perceptron with a variety of hidden nodes, trained with the resilient propagation algorithm, consistently yielded the most accurate predictions. In addition, a modeled direct normal irradiance field and adjacent weather station data were used to bolster prediction accuracy. In later trials, the solar radiation field was preprocessed with a discrete wavelet transform with the aim of removing noise from the measurements. The current model provides predictions of solar radiation with a mean square error of 0.0042, which is competitive with many of the models within the solar radiation forecasting literature.

2.2 INTRODUCTION

Solar radiation forecasting is a problem within time series prediction that has received considerable attention, as such predictions can inform the expected yield from crops in a given year or the amount of energy that can be produced from a solar panel [1]-[3]. One common model for solar radiation prediction is an artificial neural network (for examples, see [4]-[6]), as these networks serve as universal function approximators [7]. Although other models and

techniques exist for time series prediction such as support vector machines (SVM), hidden Markov models (HMM), dynamic Bayesian networks (DBN), and autoregressive integrated moving average (ARIMA) models, artificial neural networks (ANNs) have a demonstrated history of success in predicting solar radiation. Furthermore, ANNs are highly customizable in how the network can be configured (e.g. how many hidden layers/nodes, feedforward vs. recurrent, etc.), and can thus be tailored to a specific problem more readily. As solar radiation is influenced by a number of environmental and atmospheric conditions, an ANN was selected as the most appropriate model for the current study.

In the present study, a model was constructed to predict the amount of solar radiation that will make contact with the surface of the earth in a given location an hour into the future. This study was supported by the Southern Company with the idea that the model could be used to determine at what specific times during a given day of the year solar panels could be relied upon to produce energy in sufficient quantities. An artificial neural network was used to approximate the nonlinear pattern of solar radiation, which utilized measurements of weather conditions collected at the Griffin, Georgia weather station as inputs. A number of network configurations and training strategies were utilized, though a multilayer perceptron with a variety of hidden nodes trained with the resilient propagation algorithm consistently yielded the most accurate predictions. In addition, a modeled DNI field and adjacent weather station data were used, in an effort to reduce prediction error. In later trials, the solar radiation field was preprocessed with a discrete wavelet transform with the aim of removing noise from the measurements.

Direct normal irradiance (DNI) is the amount of solar radiation that will make contact with a given area under cloudless sky conditions [8]. As the actual amount of solar radiation that is measured locally has been subjected to environmental factors (e.g. cloud coverage,

atmospheric gases) before it is measured, DNI can serve as a point of comparison when analyzing solar radiation data. Thus, DNI appears to be a useful field to train an artificial neural network with for the sake of predicting the actual amount of solar radiation, as the two fields should be strongly correlated. The model in this study utilized a modeled DNI field, in conjunction with measured solar radiation, in order to predict solar radiation one hour into the future.

Discrete wavelet transform (DWT) is a technique commonly used for noise reduction in signal processing and data compression [9]. The current study treats the solar radiation field as a signal and decomposes the signal into an orthogonal set of wavelets, then reconstructs the signal with the noise removed [10]. Thus, preprocessing the solar radiation field with DWT was hypothesized to be an effective technique for improving the model's prediction accuracy. Furthermore, adjacent weather station data were added into the models' input, as prior research on solar radiation forecasting performed at UGA demonstrated performance improvements through this approach [11]. In sum, the current study aimed to assess some of the most successful prediction models and techniques demonstrated within previous studies.

2.3 MATERIALS

Data from the Griffin, Georgia weather station from 2003-2013 were used to build the observations for the input layer to the neural network. Observations were collected in 15 minute intervals over the duration of each year for a total of 35040 observations per year. Forty-three data fields were observed, though only a subset of these fields was used for solar radiation prediction: year, day of year, time of day, air temperature (°C), humidity (%), dew point (°C), vapor pressure (kPa), barometric pressure (kPa), wind speed (m/s), solar radiation (W/m^2), total

solar radiation (KJ/m^2), photosynthetically active radiation (umole/m^2s), and rainfall (mm). In later models, measurements of solar radiation from the Williamson, GA weather station - the weather station nearest to the Griffin station - were incorporated as input into the neural network, as data field measurements from nearby adjacent weather stations have been shown to improve performance of solar radiation predictions [11].

In order to further reduce prediction error, values for direct normal irradiance (DNI) were modelled for each time step. In addition to the observed fields at the Griffin station, observations of aerosol optical depth, water vapor, and Angstrom's coefficient were taken from AERONET (http://aeronet.gsfc.nasa.gov) at the Georgia Tech site, and used to calculate DNI across the different DNI models implemented. Five separate models were used to calculate the DNI field: WGEN [12], Hoogenboom's [13], Yang's model [14], Iqbal's model [15], and ESRA2 [16]-[17]. These models were selected as they have been shown to be some of the most efficacious models for modeling DNI [8], [18].

2.4 METHODS

The fields used for prediction of future solar radiation values were first extracted from the raw measurement files from the Griffin station. For each value of the extracted fields at time step *t* (with the exception of year, day, and time), values from the four previous time steps (t_{-1}, t_{-2}, t_{-3}, t_{-4}) were added to the observation file that would serve as input into the input layer of the neural network. This is known as the *sliding window technique* and has been shown to significantly increase the performance of time series predictions with neural networks [19]. In addition, delta values were calculated for each data field instance by subtracting the previous value from the current value, and were added to the observation file as well.

Modeled values of direct normal irradiance (DNI) were then calculated and added to the observation file for each time step, in addition to their corresponding previous time step and delta values. Although each model varied in the measured and modeled fields used for calculation of DNI, there were some common fields utilized in most or all of the models. The most utilized fields in calculating DNI were solar declination angle (2.1), hour angle (2.2), solar elevation angle (2.3), zenith angle (2.4), and relative air mass (2.5), as shown in equations (2.1)-(2.5):

$$DA = \sin^{-1}\left(\sin 23.25 \times \sin\left(\left(\frac{360}{365}\right) \times (day - 81)\right)\right) \quad (2.1)$$

$$HA = 15 \times (LST - 12), where\ LST\ is\ local\ solar\ time \quad (2.2)$$

$$EA = 90 - Latitude + DA \quad (2.3)$$

$$ZA = 90 - EA \quad (2.4)$$

$$m = \frac{1}{\cos ZA} \quad (2.5)$$

After the extracted data fields, the modeled DNI values, and (in later models) the solar radiation values from the Williamson station were added to the observation file, each value within the file was scaled within a range of 0 to 1, in proportion to the minimum and maximum values within their respective fields. In subsequent models, the scaled values for the solar radiation field were extracted from the observation file, processed through a discrete wavelet transform (DWT), and inserted back into the observation file. The JWave Java library was used to perform the DWT. Haars, Coiflet, Daubechie, and Legendre wavelet transforms were performed on the solar radiation field in separate trials in 1-D, 2-D, and 3-D. Once the solar radiation field was transformed and replaced within the observation file, the scaled fields were input into the neural network that was implemented using the Encog Java library.

During model development, a number of network configurations and training regimes were tested, in addition to varying combinations of input fields, in an effort to determine the

setup that would yield the most accurate solar radiation predictions. Trials began with a standard multi-layer perceptron (MLP) network configuration with 29 input nodes, 57 hidden nodes and 1 output node that provided the prediction of solar radiation one hour into the future. In subsequent trials, the number of hidden nodes was adjusted within a range of 17-257 nodes. The initial trials used air temperature, humidity, dew point, barometric pressure, wind speed, solar radiation, total solar radiation, photosynthetically active radiation, and rainfall as the input fields into the neural network. In later trials, various combinations of these fields were used. Furthermore, the backpropagation algorithm was used to train the neural network in the initial trials, but was then replaced with the resilient propagation algorithm (iRPROP+) [20]-[21] which consistently yielded more accurate predictions across network configurations.

As a recurrent neural network is not only dependent on the current input, as a MLP is, but is also dependent on previous inputs stored in the context layer [22]-[23]. As such, it was hypothesized that an Elman network would yield more accurate results than a MLP network. An Elman network with 57 hidden nodes was configured and trained with a hybrid strategy of resilient propagation and simulated annealing (SA). The following trials replaced simulated annealing with particle swarm optimization (PSO) for the training strategy. An incremental pruning regime was then implemented, which tested the mean squared error (MSE) for networks with successively larger hidden layers until the addition of hidden nodes no longer improved the MSE returned. PSO and SA were then used independently to train the Elman network after a hidden layer configuration was determined through incremental pruning.

A series of radial basis function networks (RBFNs) were then implemented for solar radiation prediction. The initial RBFN was configured with 49 hidden nodes and a Gaussian radial basis function. In the trials that followed, the centers and widths of the radial basis

functions were randomized. Subsequent networks used a Mexican Hat radial basis function and a hidden layer with hidden nodes within the range of 81-196. Singular value decomposition (SVD) was then used to train a RBFN with 196 hidden nodes.

The network type was then switched to a support vector machine with the same 29 inputs. After the SVM trials were carried out, the model was switched back to a MLP neural network with 157-207 hidden nodes and trained with the resilient propagation algorithm. Within these trials, modeled DNI values and adjacent weather station data were included, in addition to solar radiation preprocessing with DWT.

2.5 RESULTS

A MLP network with 157 hidden nodes was consistently shown to be the network configuration that yielded the most accurate solar radiation predictions. The most accurate model achieved an MSE of 0.0042 after 4000 epochs using air temperature, humidity, solar radiation (SR), total solar radiation (TSR), photosynthetically active radiation (PAR), and rainfall as the input fields (see Table 2.3 for configurations used in the experiments). The network was able to attain the same accuracy after the TSR and PAR fields were removed. Furthermore, the same network setup with air temperature, humidity, SR and DNI (WGEN model) also achieved an MSE of 0.0042. These results were obtained without preprocessing the SR data through DWT or the adjacent weather station data. The greatest accuracy of the remaining network configurations, input field combinations, and training regimes implemented are summarized in Table 2.1 and Table 2.2.

Table 2.1
Final MSE without DNI, Adjacent Stations, & DWT

Net Type	# of Hidden Nodes	Training Regime	Epochs	MSE	Notes
MLP	57	RPROP/SA	14	0.008	Greedy
Elman	57	RPROP/SA	250	0.007	Ended
Elman	57	RPROP/PSO	25	0.012	Ended
Elman	57	PSO	17	0.06	Ended
Elman	57	SA	127	0.045	Ended
Elman	5-75	RPROP, IP	10 epochs per node	0.0125	57 hidden nodes selected as best
Elman	57	RPROP	200	0.01	Ended
RBF	49	RPROP	418	0.0115	Gaussian
RBF	81	RPROP	243	0.0078	Mex. Hat
RBF	196	RPROP	716	0.00616	Mex. Hat
RBF	196	SVD	1	0.0727	Stagnant
SVM	-	-	1	0.0065	Stagnant

Table 2.2
Final MSE with DNI, Adjacent Stations, & DWT

Net Type	# of Hidden Nodes	Training Regime	Epoch	MSE	Notes
MLP	157	RPROP	2600	0.0043	AT, H, SR,DNI (WGEN)
MLP	157	RPROP	2540	0.0047	AT, H, SR, DNI (Hoogenboom)
MLP	157	RPROP	3104	0.0043	AT,H,SR,DNI (Yang)
MLP	207	RPROP	1932	0.0044	A,H,SR, AWS
MLP	207	RPROP	2500	0.0043	All, AWS,DNI (Iqbal)
MLP	207	RPROP	3600	0.0048	All, AWS, DNI (ESRA2)
MLP	207	RPROP	3510	0.0043	Same w/DWT (D2)
MLP	207	RPROP	255	0.0051	Same w/DWT (H2)

All trials shown in Tables 2.1 and 2.2 use air temperature, humidity, solar radiation and rainfall as their input fields, unless otherwise specified. It is important to note that the trials represented in Tables 2.1 and 2.2 were the best results for their respective configurations; trials

with less accurate results have not been shown. Trials involving a greedy strategy halted before the network could achieve a lower MSE, so this strategy was abandoned in subsequent trials. Simulated annealing and particle swarm optimization strategies were relatively slow to train the networks they were used upon, and would often halt before the network had completed training. The incremental pruning regime selected 57 hidden nodes as the configuration that produced the lowest MSE within a range of 5-75 hidden nodes. A larger range of hidden nodes was not tested, nor was incremental pruning implemented on a MLP. Moreover, the application of a support vector machine (SVM) showed promise by obtaining an MSE of 0.0065, but was unable to demonstrate improvement in subsequent trials.

Although the five models of DNI performed relatively the same, the WGEN consistently helped the prediction model attain a slightly lower MSE than the other models. Contrary to findings by Li et al. [11], the addition of adjacent weather station SR data did not improve prediction accuracy. Likewise, preprocessing the SR data with a DWT did not improve prediction accuracy, and in some cases, hampered it. Trials where SR data were preprocessed with Coiflet and Legendre wavelet transforms are not shown, as the resulting MSE was not within an admissible range. Tables 2.3 and 2.4 demonstrate the final MSEs obtained with various input parameters (e.g. rainfall, humidity, temperature, etc).

Table 2.3
Final MSE for 1-Hr Predictions Using Varying Input Fields

Trial	A	B	C	D	E	F	G	H	I	J	K
Day	x	x	x	x	x	x	x	x	x	x	x
Time	x	x	x	x	x	x	x	x	x	x	x
AirTemp		x									
Humid						x				x	
DewPt					x						
BarPress							x				
WindSp								x			
SR	x	x	x	x	x	x	x	x	x	x	x
TSR				x							x
PAR									x		x
Rainfall			x							x	
Prev. & Delta											
AirTemp		x									
Humid						x				x	
DewPt					x						
BarPress							x				
WindSp								x			
SR	x	x	x	x	x	x	x	x	x	x	x
TSR				x							x
PAR									x		x
Rainfall			x							x	
Best MSE ($1x10^{-3}$)	4.3	4.3	4.4	4.5	4.5	4.5	4.6	4.8	5.7	4.4	5.0

Table 2.4
Final MSE for 1-Hr Predictions Using Varying Input Fields

Trial	L	M	N	O	P	Q	R	S	T	U	V
Day	x	x	x	x	x	x	x	x	x	x	x
Time	x	x	x	x	x	x	x	x	x	x	x
AirTemp	x			x			x		x		x
Humid	x		x		x	x	x		x		x
DewPt											x
BarPress							x				x
WindSp								x			x
SR	x	x	x	x	x	x	x	x	x	x	x
TSR		x		x	x	x		x	x	x	x
PAR		x	x	x	x			x		x	x
Rainfall	x	x	x			x	x	x	x	x	x
Prev. & Delta											
AirTemp	x			x			x		x		x
Humid	x		x		x	x	x		x	x	x
DewPt											x
BarPress							x				x
WindSp								x			x
SR	x	x	x	x	x	x	x	x	x	x	x
TSR		x		x	x	x		x	x	x	x
PAR		x	x	x	x			x		x	x
Rainfall	x	x	x			x	x	x	x	x	x
Best MSE ($1x10^{-3}$)	4.2	4.9	5.0	5.2	5.4	6.0	4.3	4.5	6.2	4.2	4.6

2.6 CONCLUSION

The results of the trials summarized in Tables 2.1-2.4 suggest that the current air temperature, humidity, and solar radiation are the most vital inputs for accurately predicting solar radiation an hour into the future. This finding is intuitive, as the amount of water molecules suspended in the air influences the solar radiation that makes contact with the surface of the earth, and air temperature is an indication of the amount of solar radiation that has entered into the atmosphere and contacted the earth's surface. Rainfall and DNI also serve as accurate

predictors of solar radiation, though using both of these fields in combination did not appear to improve accuracy any more than using either field in isolation.

The MLP network with 157+ hidden nodes consistently yielded the most accurate predictions, despite other studies which have had success with recurrent networks [23], RBFNs [24], and SVMs [25]-[26]. Likewise, the resilient propagation algorithm produced the most accurate predictions across trials, in comparison to the other training strategies implemented. Despite the success of this network configuration and training regime in regularly attaining an MSE below 0.0044, the addition of modeled DNI, adjacent weather station data, and preprocessing with DWT did not improve prediction accuracy, despite success demonstrated with these techniques within the time series literature [12], [8], [10], [27]. These findings suggest that further model development is needed to make sufficiently accurate solar radiation predictions.

Despite the breadth and diversity of the network configurations, input fields, and training strategies used in this study, there are still a number of approaches that may be taken in the future in an attempt to improve prediction accuracy. For one, other measures of error such as mean absolute error (MAE) and mean absolute percentage error (MAPE) may be used to determine how the current model(s) compare with those within the solar radiation forecasting literature. Second, an autoregressive integrated moving average (ARIMA) and artificial neural network hybrid model may be implemented, as such models have demonstrated high performance in a number of other time series prediction problems [29], such as the British pound/US dollar exchange rate[28], sunspot appearance [31], and water quality [30]. Third, the equations used to calculate the modeled DNI value could be adjusted to better fit solar radiation prediction. Fourth, the current model could be tested with data from other weather stations, in

order to determine how its predictions generalize to other geographic regions. In conclusion, although the accuracy of the model was not improved beyond an MSE of 0.0042, the model remains more accurate than many models of solar radiation currently found within the literature.

2.7 REFERENCES

1. Bodri, B. (2001). A neural-network model for earthquake occurrence. *Journal of Geodynamics*, 32(3), 289-310.
2. Ball, R. A., Purcell, L. C., & Carey, S. K. (2004). Evaluation of solar radiation prediction models in North America. *Agronomy Journal*, 96(2), 391-397.
3. Thornton, P. E., Hasenauer, H., & White, M. A. (2000). Simultaneous estimation of daily solar radiation and humidity from observed temperature and precipitation: an application over complex terrain in Austria. *Agricultural and Forest Meteorology*, 104(4), 255-271.
4. Mellit, A., &Pavan, A. M. (2010). A 24-h forecast of solar irradiance using artificial neural network: Application for performance prediction of a grid-connected PV plant at Trieste, Italy. *Solar Energy*, 84(5), 807-821.
5. Elizondo, D., Hoogenboom, G., & McClendon, R. W. (1994). Development of a neural network model to predict daily solar radiation. *Agricultural and Forest Meteorology*, 71(1), 115-132.
6. Rehman, S., &Mohandes, M. (2008). Artificial neural network estimation of global solar radiation using air temperature and relative humidity. *Energy Policy*, 36(2), 571-576.
7. Hornik, K., Stinchcombe, M., & White, H. (1989). Multilayer feedforward networks are universal approximators. *Neural networks*, 2(5), 359-366.
8. Gueymard, C. A. (2003). Direct solar transmittance and irradiance predictions with broadband models. Part I: detailed theoretical performance assessment. *Solar Energy*, 74(5), 355-379.
9. Akansu, A. N., & Smith, M. J. (Eds.). (1996). Subband and wavelet transforms: design and applications (No. 340). *Springer*.

10. Jensen, A., & la Cour-Harbo, A. (2001). Ripples in mathematics: the discrete wavelet transform. *Springer*.
11. Li, B., McClendon, R. W., & Hoogenboom, G. (2004). Spatial interpolation of weather variables for single locations using artificial neural networks. *Transactions of the ASAE*, 47(2), 629-637.
12. Richardson, C.W. & Wright, D.A. (1984). WGEN: A model for generating daily weather variables. U.S. Department of Agriculture, Agricultural Research Service, *ARS-8*, 83.
13. Hoogenboom, G., Jones, J. W., Wilkens, P. W., Batchelor, W. D., Bowen, W. T., Hunt, L. A., ... & White, J. W. (1994). Crop models. *DSSAT* version, 3(2), 95-244.
14. Yang, K., Huang, G. W., &Tamai, N. (2001). A hybrid model for estimating global solar radiation. *Solar energy*, 70(1), 13-22.
15. Wong, L. T., & Chow, W. K. (2001). Solar radiation model. *Applied Energy*, 69(3), 191-224.
16. Geiger, M., Diabaté, L., Ménard, L., & Wald, L. (2002). A web service for controlling the quality of measurements of global solar irradiation. *Solar energy*, 73(6), 475-480.
17. Rigollier, C., Bauer, O., & Wald, L. (2000). On the clear sky model of the ESRA—European Solar Radiation Atlas—with respect to the Heliosat method. *Solar energy*, 68(1), 33-48.
18. Badescu, V., Gueymard, C. A., Cheval, S., Oprea, C., Baciu, M., Dumitrescu, A., & Rada, C. (2012). Computing global and diffuse solar hourly irradiation on clear sky. Review and testing of 54 models. *Renewable and Sustainable Energy Reviews*, 16(3), 1636-1656.

19. Paoli, C., Voyant, C., Muselli, M., &Nivet, M. L. (2010). Forecasting of preprocessed daily solar radiation time series using neural networks. *Solar Energy*, 84(12), 2146-2160.
20. Igel, C. &Hüsken, M. (2000) Improving the Rprop Learning Algorithm. *Second International Symposium on Neural Computation* (NC 2000), 115-121.
21. Igel,C. &Hüsken, M. (2003) Empirical Evaluation of the Improved Rprop Learning Algorithm. *Neurocomputing* 50:105-123.
22. Connor, J. T., Martin, R. D., & Atlas, L. E. (1994). Recurrent neural networks and robust time series prediction. *Neural Networks, IEEE Transactions on*, 5(2), 240-254.
23. Giles, C. L., Lawrence, S., &Tsoi, A. C. (2001). Noisy time series prediction using recurrent neural networks and grammatical inference. *Machine learning*, 44(1-2), 161-183.
24. Cheng, E. S., Chen, S., &Mulgrew, B. (1996). Gradient radial basis function networks for nonlinear and nonstationary time series prediction. *Neural Networks, IEEE Transactions on*, 7(1), 190-194.
25. Kim, K. J. (2003). Financial time series forecasting using support vector machines. *Neurocomputing*, 55(1), 307-319.
26. Thissen, U., Van Brakel, R., De Weijer, A. P., Melssen, W. J., &Buydens, L. M. C. (2003). Using support vector machines for time series prediction. *Chemometrics and intelligent laboratory systems*, 69(1), 35-49.
27. Grant, R. H., Hollinger, S. E., Hubbard, K. G., Hoogenboom, G., &Vanderlip, R. L. (2004). Ability to predict daily solar radiation values from interpolated climate records for use in crop simulation models. *Agricultural and forest meteorology*, 127(1), 65-75.

28. Zhang, G. P. (2003). Time series forecasting using a hybrid ARIMA and neural network model. *Neurocomputing*, 50, 159-175.

29. Ho, S. L., Xie, M., & Goh, T. N. (2002). A comparative study of neural network and Box-Jenkins ARIMA modeling in time series prediction. *Computers & Industrial Engineering*, 42(2), 371-375.

30. ÖmerFaruk, D. (2010). A hybrid neural network and ARIMA model for water quality time series prediction. *Engineering Applications of Artificial Intelligence*, 23(4), 586-594.

31. Khashei, M., &Bijari, M. (2011). A novel hybridization of artificial neural networks and ARIMA models for time series forecasting. *Applied Soft Computing*, 11(2), 2664-2675.

CHAPTER 3

HOURLY SOLAR RADIATION FORECASTING THROUGH MODEL AVERAGED NEURAL NETWORKS AND ALTERNATING MODEL TREES[4]

[4] Hamilton, C.R., Maier, F., & W.D. Potter. 2016. Accepted by I*nternational Conference on Industrial, Engineering & Other Applications of Applied Intelligent Systems*. Reprinted here with permission of the publisher.

3.1 ABSTRACT

The objective of the current study was to develop a solar radiation forecasting model capable of determining the specific times during a given day that solar panels could be relied upon to produce energy in sufficient quantities to meet the demand of the energy provider, Southern Company. Model averaged neural networks (MANN) and alternating model trees (AMT) were constructed to forecast solar radiation an hour into the future, given 2003-2012 solar radiation data from the Griffin, GA weather station for training and 2013 data for testing. Generalized linear models (GLM), random forests, and multilayer perceptron (MLP) were developed, in order to assess the relative performance improvement attained by the MANN and AMT models. In addition, a literature review of the most prominent hourly solar radiation models was performed and normalized root mean square error was calculated for each, for comparison with the MANN and AMT models. The results demonstrate that MANN and AMT models outperform the standard time series forecasting models, as well as most of the highest-performing models within the literature, while competing with the remaining models. MANN and AMT are thus promising time series forecasting models that may be further improved by combining these models with the top performing within the literature.

3.2 INTRODUCTION

With the world population projected to increase to 9.6 billion by 2050 [33], there is an urgent need to utilize renewable energy sources. The necessity of harnessing renewable energy is more apparent when one considers that the average farm uses 3 kcal of fossil fuel energy to produce 1 kcal of food energy before that food is even processed or transported to the market [12]. In order to ensure that the energy needs of a population are met, it is vital that there are

systems in place for forecasting how much energy can be anticipated in the future, such that usage of non-renewable energy resources can be scaled back accordingly. Thus, a highly accurate model of solar radiation prediction is imperative as such predictions can inform the expected yield from crops in a given year as well as the amount of energy that will be produced from a solar panel at a given location and time [12], [16]. The present study proposes a model for hourly solar radiation prediction whose performance is competitive with the leading models of solar radiation (compare with [3], [29], and [31]).

With the ability to predict the amount of solar energy that will be produced by a set of solar panels, assuming a constant efficiency of the panels, it is possible for energy providers to reduce their usage of non-renewable energy resources. The forecasting model utilized measurements of weather conditions collected at the Georgia Automated Environmental Monitoring Network's (GAEMN) Griffin weather station as inputs. As shown in Figures 3.1 and 3.2, the overall trend of increasing solar radiation through the spring and summer, and the decrease starting in the fall, is present in the solar radiation data from year to year. However, the amount of solar radiation occurring on a given day at a given time can vary drastically between years, which prevents linear approximation techniques from yielding accurate predictions. In order to model the nonlinearity present within the data, a number of machine learning models were implemented including least median squares, random forest, alternating model trees [6], and artificial neural networks.

To further bolster prediction accuracy, model averaged neural networks were constructed from combinations of single networks with the same architecture, but with their respective weight vectors initialized randomly to distinct sets of values. It was conjectured that since the final weight vector for a network is deterministic, given its initial weight vector, the training set,

and the learning algorithm, a greater extent of the search space for the weight vector could be explored by creating multiple copies of the same network, but with different initial weights. It was hypothesized that the average of the outputs from these networks would be closer to the global optimum, as more of the weight space would be explored by initializing each network with a distinct weight vector. This is to say that by initializing the networks to different weights, training each network on the same time series, and averaging their output would help reduce the bias inherent in any network's initial weights. As a consequence, the model averaged neural network should have a smaller mean square error for its predictions, in comparison to a single neural network [32]. Thus, the model averaged neural network appears to be an effective approach for improving the accuracy of continuous value predictions, such as the amount of solar radiation to occur, when compared to a single neural network.

Alternating model trees (AMTs) were also implemented, due to their demonstrated efficacy in time series domains [6]. Two nodes comprise AMTs: splitter nodes, where numeric attributes are split at the median value of the attribute, and predictor nodes, which utilize linear regression to predict the numeric output at that node. In addition, an AMT is grown via forward stage-wise additive modeling, where the residual errors made by the current AMT are fitted to a base learner (e.g. a decision stump or a linear regression model), after which the fitted base learner is added into the regression predictions made by the AMT. The AMT is tuned by specifying the number of iterations to grow the tree for (i) as well as the shrinkage (λ), which dampens the predictions of each base learner within the additive model towards predicting the mean of the target series. Thus, an AMT was deemed appropriate for the domain of solar radiation, as the replacement of constant values with linear regression models at the leaf nodes of the decision tree allow AMTs to model non-linear curves in a piece-wise fashion.

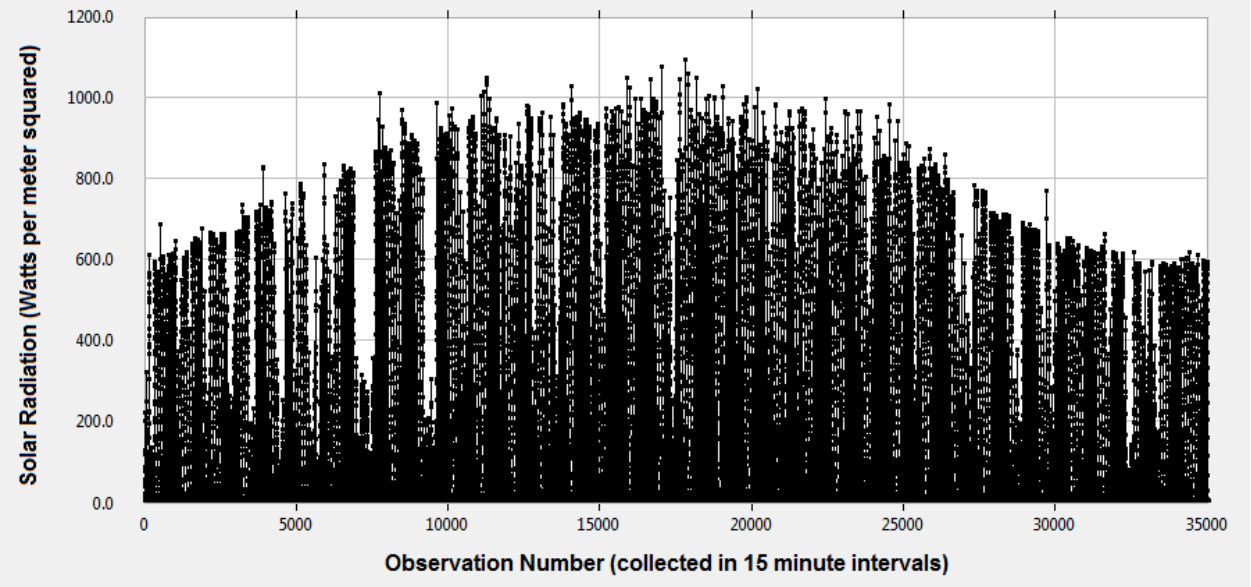

Figure 3.1. Solar radiation data collected in 15 minute intervals from the Griffin, Georgia weather station in 2003.

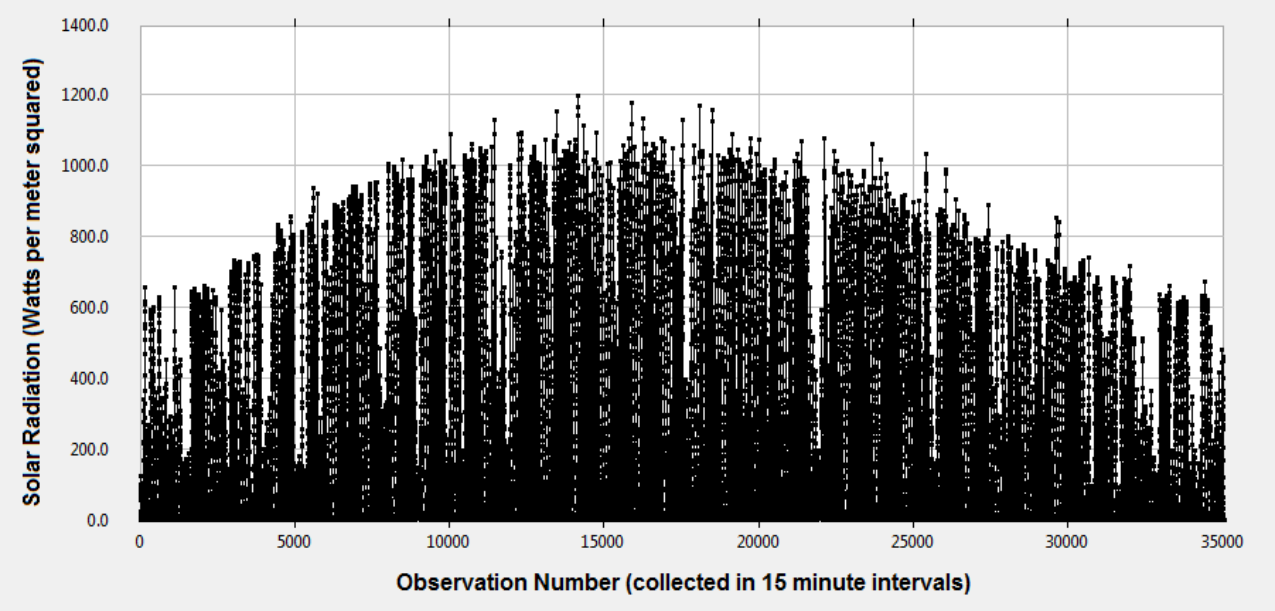

Figure 3.2. Solar radiation data collected in 15 minute intervals from the Griffin, Georgia weather station in 2013.

3.3 LITERATURE REVIEW

Sfetsos & Coonick [29] evaluated several model types, including a linear regression model, Elman networks (ELM), radial basis function networks (RBF), adaptive neuro-fuzzy inference systems (ANFIS), and neural networks trained using backpropagation (BP) and the Levenberg-Marquardt (LM) algorithm. Of these algorithms, the LM algorithm attained the smallest error, likely due to the fact that it combines gradient descent (backpropagation) and Newton's method, and thus has the strengths of both [8],[19],[21]. The LM algorithm is described by equation (3.1):

$$W_{min} = W_0 - (H + \lambda I)^{-1} g \tag{3.1}$$

Within equation (3.1), W_0 is the weight matrix of the neural network, H is the Hessian matrix, λ is the damping factor, I is the identity matrix, and g represents the gradients of the neural network. Their study indicated that a neural network trained with the LM algorithm provided superior predictions to the other models, with an RMSE of 27.58 Wm^{-2}.

Mellit and colleagues [22] implemented an artificial neural network and Markov transition matrix (MTM)[5] hybrid model to achieve daily solar radiation predictions with an mean absolute percentage error (MAPE) not exceeding eight percent. Spokas and Forcella's [30] model predicted hourly solar radiation as the sum of direct beam radiation and diffuse solar radiation; these values were calculated based upon the angle between the sun's location and the earth's surface (i.e. the zenith angle), the seasonal variability of the Earth's tilt (i.e. declination angle), the percentage of direct radiation passes through the atmosphere without being reflected (i.e. atmospheric transmittance), and the optical air mass number. Spokas and Forcella's model

[5] A Markov transition matrix is a matrix which characterizes the transitions of a Markov chain [1]. For a given element *i,j* describes the probability of moving from state *i* to state *j* in one time step. It is also known as a probability matrix, substitution matrix, or a stochastic matrix.

provided estimations of hourly solar radiation with an RMSE ranging from 77 – 167 Wm^{-2} (M = 112 Wm^{-2}) and a mean absolute error from 36 – 92 Wm^{-2} (M = 57 Wm^{-2}) across 18 sites between the years 1996–2005, with a maximum observed solar radiation of 1100 Wm^{-2} . Hocaoglu, Gerek, & Kurban [9] derived a unique representation of their solar radiation data by converting the 1D time series into a 2D image signal. The value for each pixel (x, y) within the image was determined as the solar radiation that occurred on the x hour of the y^{th} day of the year. The solar radiation values were scaled within the range 0-255, such that the corresponding pixel had a value of 0 if no solar radiation occurred and a value of 255 if the maximum amount of solar radiation within the dataset occurred. A 3-3-1 neural network was then trained on the resulting input representation. Hocaoglu, Gerek, & Kurban confirmed that the LM algorithm also yielded the most accurate predictions of all the training algorithms applied, with a resulting RMSE of 34.57 Wm^{-2}, given a maximum observed solar radiation of 600 Wm^{-2}. Thus, the 2-D representation of the input data was a significant improvement upon the 1-D representation, which achieved a RMSE of 43.73 Wm^{-2} with the same network architecture and training algorithm. More recently, the resilient propagation algorithm has been shown to outperform LM on some solar radiation data [7].

Cao & Lin [3] implemented a diagonal recurrent wavelet neural network (DRWNN), which is a recurrent neural network that uses wavelet bases as its activation functions. The DRWNN was trained on a year of solar radiation data and attained an RMSE of 13.2 Wm^{-2} when tested on a month of data. Ji and Chee [18] implemented a novel hybrid model that aggregated the outputs of an autoregressive moving average (ARMA) model and a time delay neural network (TDNN) in order to determine its prediction of hourly solar radiation.

One of the reoccurring problems within the literature on solar radiation forecasting is the lack of unity in performance metrics for comparing models. As Hoff et al. [11] note, while RMSE and mean absolute error (MAE) are calculated with the same equation across studies, their calculations as percentages are not. The most apparent case is with calculations of normalized RMSE (NRMSE). Equations (3.2) and (3.3) demonstrate the two most common formulations of NRMSE:

$$NRMSE = \frac{RMSE}{y_{max} - y_{min}} = \frac{\sqrt{\frac{\sum_{i=1}^{n}(\hat{y}_i - y_i)^2}{n}}}{y_{max} - y_{min}} \tag{3.2}$$

$$NRMSE = \frac{RMSE}{\bar{y}} = \frac{\sqrt{\frac{\sum_{i=1}^{n}(\hat{y}_i - y_i)^2}{n}}}{\bar{y}} \tag{3.3}$$

It is necessary to calculate a normalized RMSE when comparing models, as RMSE itself is not calculated with respect to scale of the predicted value across models. For instance, suppose model A achieves a RMSE of 15 W/m^2 on a dataset with an $\bar{y}$ = 250, y_{min} = 0 W/m^2 and y_{max} = 400 W/m^2. In contrast, model B achieves a RMSE of 30 W/m^2 on a dataset with an $\bar{y}$ = 500 W/m^2, y_{min} = 0 W/m^2 and y_{max} = 1000 W/m^2. If equation (3.2) is used to calculate NRMSE for models A and B, then model B will be characterized as the more accurate model as 15/400-0 = 0.0375 and 30/1000-0 = 0.03, respectively. However, if equation (3.3) is used to calculate NRMSE (often referred to as coefficient of variation of the RMSE), models A and B can be said to have equal performance as 15/250 = 30/500 = 0.06. Thus, a single equation should be used to calculate NRMSE for the models to be assessed, so that the comparison between them is fair. Within the current study, equation (3.2) is used to calculate NRMSE as the maximum and minimum values for solar radiation are more readily available within the literature than average solar radiation.

Table 3.1
A performance comparison between hourly solar radiation forecasting models prominent within the literature, measured as normalized root mean square error (NRMSE)

Authors	**Model Type**	**Max W/m^2 Observed**	**RMSE W/m^2**	**NRMSE (%)**
Sfetsos & Coonick (2000)	ANN trained with LM	1000	27.6	2.8
Spokas & Forcella (2006)	Clear Sky/ Direct Normal Irradiance model	1100	112	10.2
Cao & Lin (2008)	Diagonal recurrent wavelet neural network (DRWNN)	558	13.2	2.4
Hocaoglu, Gerek, & Kurban (2008)	ANN trained with 2D visual representation of time series and LM	600	34.57	5.8
Reikard (2009)	ARIMA	1100	322.3	29.3
Perez et al. (2010)	Cloud motion vectors derived from difference in consecutive GHI Index grids	1000	87.57	8.8
Marquez (2011)	ANN w/ input selection via genetic algorithm	1000	72	7.2
Izgi et al. (2012)	ANN w/ air temp., cell temp., and solar radiation as input	400	55	13.8
Pedro & Coimbra (2012)	ANN w/ parameter optimization via genetic algorithm	1000	131	13.1
Wang et al. (2012)	ANN w/ statistical feature parameters (ANN-SFP)	1200	63.5	5.3
Huang et al. (2013)	Coupled autoregressive dynamical systems (CARDS)	1146	80.6	7
Benmouiza & Cheknane (2013)	Hybrid k-means and NARX neural network model	950	64.3	6.8
Fidan, Hocaoglu, & Gerek (2014)	ANN w/ periodic Fourier series coefficients as input	400	64.3	16.1

Before interpreting the results of these forecasting studies, it is important to note several assumptions and caveats associated with the comparison of these studies/models. First, a number

of studies either did not report RMSE explicitly or provided measurements in units other than W/m^2. Models that did not have MSE/RMSE calculations within the respective article were excluded, as there was generally not enough additional information within these articles to calculate RMSE manually. Metrics such as mean absolute percentage error (MAPE), mean bias error (MBE), mean absolute error (MAE), and relative absolute error (RAE) occurred within some publications, but without enough of a consensus to warrant their use for comparing models. In addition, many articles did not specify explicit values for overall RMSE on the test set, but instead displayed error trend plots. In these cases, the error trend was averaged over time in order to determine a scalar value for RMSE for the model. Furthermore, some studies reported RMSE on a seasonal or monthly basis. The assumption was made that there was likely a uniform distribution of instances within these subsets, such that the overall RMSE of the model could be calculated as the model's average RMSE on the respective subsets.

The central difficulty in calculating NRMSE for these models is the rarity in which authors explicitly provided values for y_{min} and y_{max}. However, y_{min} was assumed to be equal to zero, while the remaining y_{max} values for these respective models was either extracted from figures within the given publication or from other metrics therein provided. In addition, some publications reported NRMSE, but did not report how normalization was performed. Future publications could be greatly improved not only by providing RMSE calculations, but also the range of values for the target variable (i.e. y_{min} and y_{max}), the average target value ($\bar{y}$), and the normalization method/formula used, in addition to other performance metrics.

Table 3.1 appears to demonstrate that Sfetsos & Coonick's (2000) feedforward neural network trained with the LM algorithm and Cao & Lin's (2008) diagonal recurrent wavelet neural network are the top performing models, as they have achieved the lowest NRMSE, in

comparison to the other models accounted for within the solar radiation forecasting literature. However, these models also highlight a further problem with comparing models between studies: there are sometimes significant differences in the size of the training and testing sets between models. Both Sfetsos & Coonick and Cao & Lin's models were tested on a dataset spanning a month or less, which suggests it is inappropriate to assume these models accurately predict solar radiation for the remaining months of the year, without further evaluation. In a similar vein, there is no sense in which solar radiation data sets across distinct studies can be treated as equivalent, as one data set may contain a significant amount of noise, due to recording equipment error or other factors, in comparison to another data set. Therefore, in order to further ensure the validity of model comparison between studies, standard baseline models such as a persistence model, where y_{t+1} is predicted as equal to y_t, should be used for determining how the proposed model improves upon the baseline model. In sum, despite the aforementioned limitations, these models serve as a basis of comparison to illustrate the efficacy and precision of models developed within the current study.

3.4 MATERIALS

Data from the Griffin, Georgia weather station from 2003-2013 were used to build the observations for the input layer to the neural network. Observations were collected at 15 minute intervals over the duration of each year for a total of 35,040 observations per year (350,400 observations total). Forty-three data fields were observed, though only a subset of these fields was used for solar radiation prediction: year, day of year, time of day, air temperature (°C), humidity (%), dew point (°C), vapor pressure (kPa), barometric pressure (kPa), wind speed (m/s), solar radiation (W/m^2), total solar radiation (KJ/m^2), photosynthetically active radiation

(umole/m^2s), and rainfall (mm). As subsequent tests of the model demonstrated that these fields did not bolster forecasting performance, only solar radiation and its respective lag were used as inputs within the models of this study.

3.5 METHODS

The fields used for prediction of future solar radiation values were first extracted from the raw measurement files from the Griffin station. For each value of the extracted fields at time step *t* (with the exception of year, day, and time), values from the n previous time steps (t_{-1}, t_{-2}, t_{-3}, …, t_{-n}) were added to the observation file that would serve as input into the input layer of the neural network. This is known as the *sliding window technique* and has been shown to significantly increase the accuracy of time series predictions with neural networks [23]. Trials to determine the optimal network architecture, input fields, and hyperparameter configuration began with a standard multilayer perceptron (MLP) network with 57 hidden nodes and 1 output node that provided the prediction of solar radiation one hour into the future. The number of nodes in the input layer of each network was determined by equation (3.4):

$$\#\ input\ nodes = n + \#\ input\ fields\ used \tag{3.4}$$

In subsequent trials, the number of hidden nodes was adjusted within a range of 17-257 nodes. The initial trials used air temperature, humidity, dew point, barometric pressure, wind speed, solar radiation, total solar radiation, photosynthetically active radiation, and rainfall as the input fields into the neural network. Combinations of these fields were then implemented, in order to determine which fields consistently provided for predictions with the lowest MSE. In later trials, only solar radiation at *t* and prior solar radiation values from t_{-1} to t_{-n} were used as input, as other

input fields did not appear to positively influence the models' performance. The activation function for this network type is formalized as shown in (3.5):

$$a_j^l = \sigma\left(\sum_k w_{jk}^l a_k^{l-1} + b_j^l\right) \tag{3.5}$$

In equation (3.5), a_j^l is the activation of the jth neuron in the lth layer, as determined by activation of neurons within the $(l_{-1})^{th}$ layer [5]. The sum $\sum_k w_{jk}^l a_k^{l-1}$ is the total activation of each neuron *k* in the $(l_{-1})^{th}$ multiplied by their respective weighted connections to each neuron *j* in the lth layer. The term b_j^l is the bias value of neuron *j* in the l^{th} layer. For each training instance d within the training set D_{train}, where $d \in D_{train}$, the weights of the network were updated through the backpropagation algorithm as shown in equation (3.6) [8].

$$\Delta w_{(t)} = \epsilon \frac{\partial E}{\partial w_{(t)}} + \alpha \Delta w_{(t-1)} \tag{3.6}$$

Thus, the change of a given weight at iteration t ($\Delta w_{(t)}$) is equal to the product of the learning rate (ϵ) and the gradient ($\frac{\partial E}{\partial w_{(t)}}$), in addition to the product of momentum (α) and the change of that weight at the previous time step ($\Delta w_{(t-1)}$).

In subsequent trials, the backpropagation algorithm was replaced with the resilient propagation algorithm (iRPROP+) [14]-[15]. The RPROP and backpropagation algorithms are similar in that gradients must be calculated for each weight, however the gradient used in RPROP is the inverse of the gradient used in backpropagation, and the RPROP gradients are utilized such that specifying a learning rate and momentum is not required [8],[27]. First, the gradient of the current iteration is compared with the gradient of the previous iteration. The calculation of sign change is shown in equation (3.7):

$$c = \frac{\partial E^{(t)}}{\partial w_{ij}} \cdot \frac{\partial E^{(t-1)}}{\partial w_{ij}} \tag{3.7}$$

The value of c is then used to determine the weight change, such that c is greater than 0, than the weight change is equal to the negative of the weight update value and positive if c is less than 0. Otherwise, no change is made to the weight. The update value for weight w_{ij} is shown in equation (3.8):

$$\Delta_{ij}^{(t)} = \begin{cases} \eta^{+} \cdot \Delta_{ij}^{(t-1)}, \ if\ c > 0 \\ \eta^{-} \cdot \Delta_{ij}^{(t-1)}, \ if\ c < 0 \\ \Delta_{ij}^{(t-1)}, otherwise \end{cases} \tag{3.8}$$

Within equation (3.8), η^{-} and η^{+} are constant parameters specified prior to training, typically with the values 0.5 and 1.2, respectively. As only the sign of the gradient is used to determine the weight update value, rather than considering the gradient itself as in backpropagation, RPROP is able to train much faster than backpropagation.

A model averaged neural network (MANN) was constructed by initializing a number of MLPs with identical architectures, but distinct weight vectors, and training these networks in parallel using the resilient propagation algorithm. The MANN was first formalized by Ripley [28]. In effect, a MANN is a voting ensemble of MLPs. The implementation of the algorithm is straightforward: first, *N* neural networks are initialized with the same architecture, and for each weight vector w_{ij} between layers *i* and *j* of network *n*, the weights are randomized using a different seed than what was used to initialize the weight vectors of the other networks. Each of the networks is trained in parallel until the minimum gradient for each network is reached. Within the present study, training was configured to continue while: 1. The training error was greater than the specified maximum acceptable error, 2. The number of epochs was less than the specified maximum number of epochs, and 3. The testing error continued to decrease from the previous testing epoch. A testing iteration was performed every 100 training iterations to ensure the network did not overfit. If any of these three conditions were violated, training of that

network was halted. Once the training of each network was complete, the networks were tested as a single MANN. The error for testing iterations was calculated by averaging the predictions of each network and then finding the difference between this average predicted value and the actual value of the output for the given testing instance. After the training of each network is complete, predictions from the MANN were simply calculated as the average of the predicted output from each network for a given instance in the data.

It is critical to note that weights of the networks comprising the MANN implemented in the current study are not updated based on the error of the MANN's predicted output value, but rather based on each network's individual error. Were the weights of each network updated based on the error of the MANN's predicted output value, the weight updates of each network would likely not shift the error function of the MANN's predictions towards a global or local minima, as the error of the MANN may differ substantially from an individual network comprising it. For instance, one of the networks comprising the MANN may be predicting values lower than the actual values, while another network within the MANN may be providing higher than the actual values. Though this example is somewhat of a simplification, it demonstrates the need to update networks within the MANN based on their individual error. In addition to MANN, generalized linear models (GLM), least median squares (LMS), random forests (RF), and alternating model trees (AMT)[6] were implemented. Like the single MLP and MANN implemented, variations in the lag input into the respective models was varied to minimize prediction error. To further optimize model performance, the number of trees used in the RF models, and the shrinkage (λ) and the number of iterations (i) used in the AMTs were varied.

[6] A detailed explanation of the alternating model tree algorithm is contained within Frank, Mayo, & Kramer (2015).

3.6 RESULTS

The MANN architecture consistently outperformed single neural network models in predicting hourly solar radiation, as shown in Table 3.2. However, the number of networks within the MANN did not appear to have a significant effect upon the RMSE of predictions when forecasts of two or more networks were averaged. In fact, prediction accuracy marginally decreased when the number of networks comprising the MANN exceeded five. One possible explanation for this phenomenon is that larger MANN may overfit the training data, such that their performance on the testing data is not improved in comparison to MANN comprised of fewer networks. This explanation is supported by observations of MANN comprised of six or more networks forecasting with a scaled MSE less than 0.0018 (<50.91 W/m^2) on training data, while MANN comprised of 5 or less networks forecasting with a scaled MSE greater than 0.0020 (>53.67 W/m^2) on training data.

Table 3.2
A comparison of the best performance of single neural networks (MLP) and model averaged neural networks (MANN) with varied amounts of lag with respect to solar radiation. The results shown are the observations taken from a given model for its best performance over five trials.

Model	**Lag**	**Scaled MSE**	**RMSE (W/m^2)**	**NRMSE (%)**
MLP	16	0.00434	79.05	6.59
MLP	96	0.00280	63.50	5.29
MANN(2)	96	0.00274	62.81	5.23
MANN(3)	96	0.00274	62.81	5.23
MANN(5)	96	0.00274	62.81	5.23
MANN(8)	96	0.00275	62.93	5.24
MANN(10)	96	0.00275	62.93	5.24

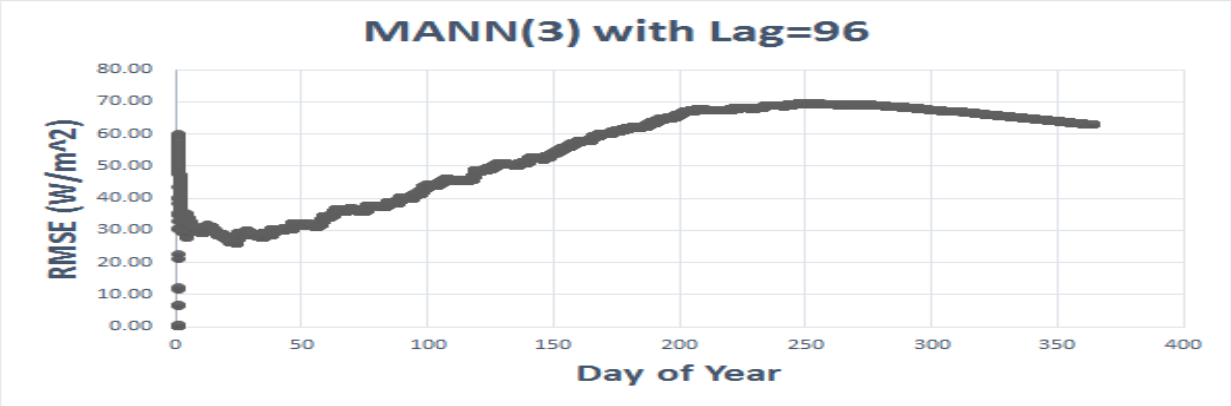

Figure 3.3. RMSE (Wm^{-2}) of the MANN(3) model with a lag of 96 on the Griffin 2013 data set.

The model achieves an RMSE of 26 Wm^{-2} on Day 24, which equates to an NRMSE of 2.2%. In addition, the average RMSE for January is 29.8 Wm^{-2} , which equates to an NRMSE of 2.5%. The performance of the MANN is thus competitive with the top models reviewed: Sfetsos & Coonick [29] and Cao & Lin [3].

Two unexpected observations can be made about the generalized linear model: first, it significantly outperformed the MLP with same amount of lag, despite the non-linear nature of the data (see Table 3.3). To understand this discrepancy in expectation, it is important to note that the GLM implemented ridge regression according to equation (3.9):

$$\beta_\gamma = \left(Z^T Z + \gamma I_p\right)^{-1} Z^T y \tag{3.9}$$

Within equation (2.9) β_γ is the vector of coefficients of the model (i.e. the weight vector), Z is the standardized (i.e. zero mean, unit variance) training data input matrix, y is the centered training data output vector, and γ is the tuning parameter [10]. The tuning parameter thus regularizes β_γ (i.e. prevents β_γ from growing too large), such that the variance of β_γ is reduced while some bias is introduced, therefore reducing overall prediction error.

The second observation is the high prediction accuracy of the AMT models in comparison to both the neural network and non-neural network models. The AMT with lag=64, the number of

boosting iterations (i)=20, and shrinkage (λ)=1.0 attained a marginally lower RMSE (62.7 W/m^2) than the MLP and MANN models, which utilized a lag of up to 96 time steps. As AMT also tend to increase in prediction accuracy with a greater amount of lag used, it is possible that a lower RMSE could be attained by further exploring the parameter space defined by i and λ.

Table 3.3
A comparison of the performance of generalized linear model (GLM), least median squares (LMS), random forest (RF), and alternating model trees (AMT) across varied amounts of lag

Model	**Lag**	**MAE**	**RRSE**	**DA**	**RAE**	**MSE**	**RMSE**	**NRMSE**
LMS	12	31.6	105.7	41	103.4	5561.3	74.6	6.22
GLM	16	34.4	94.9	42.5	112.6	4482.3	66.9	5.58
RF 100 trees	16	29.9	92.9	63.3	98	4296.1	65.5	5.46
AMT i = 10 λ = 1.0	12	27.6	92	67.2	90.4	4209.9	64.9	5.41
AMT i = 10 λ = 1.0	16	26.6	91	60.6	87.1	4118.8	64.2	5.35
AMT i = 20 λ = 1.0	16	**25.9**	89.8	60.3	**84.9**	4014.4	63.4	5.28
AMT i = 10 λ = 1.0	24	28.1	90.5	54.2	92.1	4082	63.9	5.33
AMT i =20 λ = 1.0	32	26.4	89.1	**70.1**	86.5	3955.5	62.9	5.24
AMT i = 30 λ = 0.1	32	33.6	92.7	49.4	110	4281.4	65.4	5.45
AMT i = 30 λ = 1.0	32	26	**88.8**	69.6	85.2	3929.5	**62.7**	**5.23**
AMT i = 20 λ = 1.0	64	26.2	**88.8**	51	85.6	**3928.4**	**62.7**	**5.23**

3.7 CONCLUSION

The model averaged neural network (MANN) and the alternating model tree (AMT) models were shown to produce hourly predictions of solar radiation with the least error of the models assessed within the current study. Furthermore, MANN and AMT outperform, or are competitive with, the leading models of hourly solar radiation forecasting within the literature. The increase in performance of the MANN, in comparison to single neural networks, is likely due to the capacity for a MANN to explore more of the weight space for units within its hidden layers, as it is composed of multiple networks with different initial weights but identical architectures. However, aggregating the predictions of more than two networks did not appear to improve prediction performance (i.e. reduce prediction error), though it is possible these networks were overfit due to their significantly lower prediction error on the training data. In order to further bolster prediction performance in future studies, a more rigorous stopping strategy should be implemented, where a separate weight vector of a given network is saved for t time steps, such that if training is permitted to continue for t time steps after the first instance of the testing error increasing, the weights of the network can be reverted to their values t time steps back from the current time step. Prediction performance may be further improved by using a greater lag for both MANN and AMT models, as well as by aggregating these models into an ensemble model. As decision trees and neural networks have radically different methods for attaining their model, it is likely the aggregation of their predictions will help to alleviate the shortcomings of both model types [32].

3.8 REFERENCES

1. Asmussen, S. R. (2003). "Markov Chains". *Applied Probability and Queues.* Stochastic Modelling and Applied Probability **51**. pp. 3–8.
2. Benmouiza, K., & Cheknane, A. (2013). Forecasting hourly global solar radiation using hybrid k-means and nonlinear autoregressive neural network models. *Energy Conversion and Management, 75,* 561-569.
3. Cao, J., & Lin, X. (2008). Study of hourly and daily solar irradiation forecast using diagonal recurrent wavelet neural networks. *Energy Conversion and Management, 49*(6), 1396-1406.
4. Elizondo, D., Hoogenboom, G., & McClendon, R. W. (1994). Development of a neural network model to predict daily solar radiation. *Agricultural and Forest Meteorology, 71*(1), 115-132.
5. Fidan, M., Hocaoğlu, F. O., & Gerek, Ö. N. (2014). Harmonic analysis based hourly solar radiation forecasting model. *IET Renewable Power Generation, 9*(3), 218-227.
6. Frank, E., Mayo, M., & Kramer, S. (2015). Alternating Model Trees. In *Proceedings of the 30th Annual ACM Symposium on Applied Computing*, 871-878.
7. Hamilton, C., Potter, W. , Hoogenboom, G. , McClendon, R., & Hobbs, W. (2015). 'Solar Radiation Time Series Prediction'. *International Journal of Computer, Control, Quantum and Information Engineering*, 9(5), 656 - 661.
8. Heaton, J. (2011). Introduction to the Math of Neural Networks. Heaton Research, Inc.
9. Hocaoğlu, F. O., Gerek, Ö. N., & Kurban, M. (2008). Hourly solar radiation forecasting using optimal coefficient 2-D linear filters and feed-forward neural networks. *Solar Energy, 82*(8), 714-726.

10. Hoerl, A. E., & Kennard, R. W. (1970). Ridge regression: Biased estimation for nonorthogonal problems. *Technometrics*, 12(1), 55-67.
11. Hoff, T. E., Perez, R., Kleissl, J., Renne, D., & Stein, J. (2013). Reporting of irradiance modeling relative prediction errors. *Progress in Photovoltaics: Research and Applications*, *21*(7), 1514-1519.
12. Horrigan L, Lawrence RS, Walker P (2002) How sustainable agriculture can address the environmental and human health harms of industrial agriculture. *Environmental Health Perspectives* 110: 445–456.
13. Huang, J., Korolkiewicz, M., Agrawal, M., & Boland, J. (2013). Forecasting solar radiation on an hourly time scale using a Coupled AutoRegressive and Dynamical System (CARDS) model. *Solar Energy*, *87*, 136-149.
14. Igel, C. & Hüsken, M. (2000) Improving the Rprop Learning Algorithm. *Second International Symposium on Neural Computation* (NC 2000), 115-121.
15. Igel,C. & Hüsken, M. (2003) Empirical Evaluation of the Improved Rprop Learning Algorithm. *Neurocomputing* 50:105-123.
16. Intergovernmental Panel on Climate Change. (2015). *Climate Change 2014: Impacts, Adaptation, and Vulnerability*. Geneva, Switzerland.
17. Izgi, E., Öztopal, A., Yerli, B., Kaymak, M. K., & Şahin, A. D. (2012). Short–mid-term solar power prediction by using artificial neural networks. *Solar Energy*, *86*(2), 725-733.
18. Ji, W., & Chee, K. C. (2011). Prediction of hourly solar radiation using a novel hybrid model of ARMA and TDNN. *Solar Energy*, *85*(5), 808-817.
19. Levenberg, K. (1944). A method for the solution of certain non–linear problems in least squares. *Quarterly of Applied Mathematics*, 2, 164-168.

20. Marquez, R., & Coimbra, C. F. (2011). Forecasting of global and direct solar irradiance using stochastic learning methods, ground experiments and the NWS database. *Solar Energy*, *85*(5), 746-756.
21. Marquardt, D. W. (1963). An algorithm for least-squares estimation of nonlinear parameters. *Journal of the Society for Industrial & Applied Mathematics*, *11*(2), 431-441.
22. Mellit, A., Menghanem, M., & Bendekhis, M. (2005, June). Artificial neural network model for prediction solar radiation data: application for sizing stand-alone photovoltaic power system. In *Power Engineering Society General Meeting, 2005. IEEE* (pp. 40-44). IEEE.
23. Paoli, C., Voyant, C., Muselli, M., & Nivet, M. L. (2010). Forecasting of preprocessed daily solar radiation time series using neural networks. *Solar Energy*, 84(12), 2146-2160.
24. Pedro, H. T., & Coimbra, C. F. (2012). Assessment of forecasting techniques for solar power production with no exogenous inputs. *Solar Energy*, *86*(7), 2017-2028.
25. Perez, R., Kivalov, S., Schlemmer, J., Hemker, K., Renné, D., & Hoff, T. E. (2010). Validation of short and medium term operational solar radiation forecasts in the US. *Solar Energy*, *84*(12), 2161-2172.
26. Reikard, G. (2009). Predicting solar radiation at high resolutions: A comparison of time series forecasts. *Solar Energy*, *83*(3), 342-349.
27. Riedmiller, M. (1994). *Rprop-Description and Implementation Details: Technical Report*. Inst. f. Logik, Komplexität u. Deduktionssysteme.
28. Ripley, B. (1996). *Pattern recognition and neural networks*. Cambridge University Press.
29. Sfetsos, A., & Coonick, A. H. (2000). Univariate and multivariate forecasting of hourly solar radiation with artificial intelligence techniques. *Solar Energy*,*68*(2), 169-178.

30. Spokas, K., & Forcella, F. (2006). Estimating hourly incoming solar radiation from limited meteorological data. *Weed science*, 54(1), 182-189.
31. Wang, F., Mi, Z., Su, S., & Zhao, H. (2012). Short-term solar irradiance forecasting model based on artificial neural network using statistical feature parameters. *Energies*, *5*(5), 1355-1370.
32. Witten, I., Frank, E., & Hall, M. (2011). *Data Mining: Practical Machine Learning Tools and Techniques*. Los Altos, USA: Morgan Kaufmann.
33. World Population Prospects, the 2012 Revision. (2012). Retrieved April 5, 2015, from http://esa.un.org/wpp/

CHAPTER 4

CONCLUSION AND FUTURE DIRECTIONS FOR HOURLY SOLAR RADATION FORECASTING

4.1 CONCLUSION

The results of the primary study characterized in Chapter 2 demonstrate how an artificial neural network and a model for direct normal irradiance (DNI) can be combined in order to accurately forecast hourly solar radiation. The DNI model by itself, however, was not sufficient for forecasting solar radiation within an acceptable range of error, nor were many of the other predictive models constructed, including Elman and radial basis function networks. In addition, methods including the use of solar radiation values from adjacent weather stations, preprocessing the data via a discrete wavelet transform, and training the model with the remaining input fields not described within the trials of the primary study were unable to bolster the performance of the neural network. In Chapter 3, the neural network architecture developed within the primary study was replicated with an unique initial weight vector multiple times to form an ensemble of networks. The networks comprising ensemble were trained in parallel and predictions on the test set were calculated as the average between the individual predictions made by each network. This voting ensemble method, referred to as a *model averaged neural network* (MANN) [1], attained a significantly lower RMSE (62.81 W/m^2), in comparison to a single neural network (63.50 W/m^2) when both models were input with a lag of 96 solar radiation values (24 hours). The proposed explanation for this finding is that by initializing each network's initial weight

vector to be unique in comparison to the other networks comprising the MANN, then the networks will necessarily explore different portions of the possible weight space with each gradient update performed. By averaging the predictions of multiple networks together for the final prediction, the individual variability within networks is dampened, resulting in a prediction with a greater probability of approximating the actual solar radiation value accurately. Furthermore, the importance of the lag length cannot be overstated: there is a strong negative correlation between the lag length and the prediction error. The RMSE attained by the single network model with a lag length equal to 4 (one hour) was significantly reduced from 77.77 W/m^2 to 63.50 W/m^2 when the lag length was extended to 96 (24 hours). As 96 was the upper bound of the lag length assessed, it is possible the prediction error may be further reduced by increasing the lag input into future models.

The *alternating model tree* (AMT) [2] exceeded expectations by attaining the lowest prediction error at 62.7 W/m^2 with a lag of 64. The efficacy of the AMT suggests that decision trees warrant further investigation as a solar radiation forecasting model. AMTs also have the advantage of greater interpretability, as the inequality on which the data are divided is shown at each splitter node, so it is clear how the solar radiation at prior time intervals influence the prediction of future solar radiation. Thus, this study demonstrated that the AMT must be assessed alongside neural networks and other predictive models when forecasting solar radiation.

By calculating a normalized root mean square error (NRMSE) for the top-performing and most cited solar radiation forecasting models within the literature, it was shown that the MANN and AMT models either outperform or parallel the performance of these models within the literature. Sfetsos & Coonick's [3] feedforward neural network trained with the Levenberg-Marquardt algorithm and Cao & Lin's [4] diagonal recurrent wavelet neural network appear to

be the top performing models, as they have achieved the lowest NRMSE, in comparison to the other models accounted for within the solar radiation forecasting literature as well as the MANN and AMT. However, Sfetsos & Coonick's and Cao & Lin's models also highlight a further problem with comparing models between studies: there are sometimes significant differences in the size of the training and testing sets between models. Both Sfetsos & Coonick and Cao & Lin's models were tested on a dataset spanning a month or less, which suggests it is inappropriate to assume these models accurately predict solar radiation for the remaining months of the year, without further evaluation. Thus, it is imperative that these models are reevaluated alongside the MANN and AMT models, in order to determine which model is most appropriate for the domain of solar radiation forecasting.

4.2 FUTURE DIRECTIONS

As the models of Chapter 3 demonstrated, it is necessary to explore how a longer lag length can be utilized by these predictive models to reduce prediction error. In addition to assessing individual models against each other, it is vital that the efficacy of ensembles of models, such as the MANN and the AMT, are assessed. As decision trees and neural networks have distinct learning processes and architectures, it is likely the aggregation of their predictions will help to reduce the bias inherent in both models [5]-[7]. Likewise, the top-performing models within the literature should be reassessed using the Griffin data set as well as aggregated with the MANN and AMT models, in order to establish a standard basis of comparison between models. Furthermore, it would be ideal to assess each model's efficacy across a number of geographical regions and topologies, in order to determine the generalizability of a given model. With respect to the objectives of Georgia Power and its parent company, Southern Power, future

models should be assessed in every location in which a solar collection facility is installed, which include areas in California, Georgia, Nevada, New Mexico, North Carolina and Texas [8]. In a more general context, it would be advantageous to have a standard solar radiation dataset or collection of data sets on which new prediction models could be assessed, in order to directly compare models within the literature. Likewise, future studies should calculate as many measures of error as occur within the literature, including but not limited to [normalized] root mean squared error, mean bias error, mean absolute error, relative absolute error, direction accuracy, and mean absolute percentage error. In addition, future studies should explicitly state the training and testing sets date ranges, the minimum and maximum solar radiation values observed, and the mean solar radiation value per observation. The inclusion of this information within reports on future studies will significantly improve the ability to compare solar radiation forecasting models and thus will catalyze their improvement.

As the MANN and AMT models of the current study have demonstrated success in hourly solar radiation forecasting, the next objective is to extend the models to forecast solar radiation 2-24 hours into the future. These forecasts can be made in one of two ways: the first method is to simply shift the training data such that its input remains the current solar radiation value and the solar radiation values contained within the specified lag interval, while the target value is the solar radiation that occurs *n* steps ahead. For instance, with the current models, if the input contains the solar radiation occurring at 2pm on a given day, the models will be trained to predict the solar radiation occurring at 3pm. However, in order to predict the solar radiation at $t + 4$ (i.e. 6pm), the first four values from the target solar radiation vector should be removed, so that the model learns the pattern that exists between the input values at time *t* and the solar

radiation value at $t + 4$. Thus, in order to have 24 hours of accurate solar radiation forecasts requires training 24 models on solar radiation data modified in this fashion.

The second method involves adding a closed loop to the output of the model, such that input for the model at each time step is the model's prediction at the previous time step. Thus, if at 2pm the model predicted 100 W/m^2 as the solar radiation expected at 3pm, then the model would utilize 100 W/m^2 as the input when predicting solar radiation at 4pm. This methodology allows the model to predict an arbitrary number of hours into the future. The drawback of this approach, however, is that a prediction error made at an earlier time step will propagate to future time steps, such that these predictions become exponentially worse. Therefore, the first method is likely the best method of predicting *n* time steps into the future, despite the complexity of developing and maintaining 24 separate models.

In sum, the individual neural network, the MANN, and the AMT developed within the studies characterized in Chapters 2 and 3 all serve as viable solar radiation forecasting models for application to dynamically planning energy source distribution within Georgia Power's operations. Their performance may be improved through aggregating their predictions through an ensemble strategy such as voting, long with the predictions from other viable models occurring within the literature. The forecast horizon may be extended to 2-24 (or longer) through the shifting method or the closed loop methods outlined above. However, due to the demonstrated success of the hourly solar radiation forecasting models developed within the current study, their utility in managing energy source distribution is predicted to be bright.

4.3 REFERENCES

1. Ripley, B. (1996). *Pattern recognition and neural networks.* Cambridge University Press.
2. Frank, E., Mayo, M., & Kramer, S. (2015). Alternating Model Trees. In *Proceedings of the 30th Annual ACM Symposium on Applied Computing*, 871-878.
3. Sfetsos, A., & Coonick, A. H. (2000). Univariate and multivariate forecasting of hourly solar radiation with artificial intelligence techniques. *Solar Energy*, 68(2), 169-178.
4. Cao, J., & Lin, X. (2008). Study of hourly and daily solar irradiation forecast using diagonal recurrent wavelet neural networks. *Energy Conversion and Management*, 49(6), 1396-1406.
5. Witten, I., Frank, E., & Hall, M. (2011*). Data Mining: Practical Machine Learning Tools and Techniques.* Los Altos, USA: Morgan Kaufmann.
6. Geman, Stuart; E. Bienenstock; R. Doursat (1992). Neural networks and the bias/variance dilemma. *Neural Computation*, 4: 1–58.
7. Bias–Variance Decomposition, In *Encyclopedia of Machine Learning*. Eds. Claude Sammut, Geoffrey I. Webb. Springer 2011. pp. 100-101.
8. Southern Company. (2016). Renewable Resources. Retrieved April 08, 2016, from http://www.southerncompany.com/what-doing/corporate-responsibility/energy-innovation/building-renewable-resources.cshtml#solar

CHAPTER 5

BIBLIOGRAPHY

Akansu, A. N., & Smith, M. J. (Eds.). (1996). *Subband and wavelet transforms: design and applications* (No. 340). Springer.

Asmussen, S. R. (2003). "Markov Chains". *Applied Probability and Queues.* Stochastic Modelling and Applied Probability **51**. pp. 3–8.

Badescu, V., Gueymard, C. A., Cheval, S., Oprea, C., Baciu, M., Dumitrescu, A., & Rada, C. (2012). Computing global and diffuse solar hourly irradiation on clear sky. Review and testing of 54 models. *Renewable and Sustainable Energy Reviews*, 16(3), 1636-1656.

Ball, R. A., Purcell, L. C., & Carey, S. K. (2004). Evaluation of solar radiation prediction models in North America. *Agronomy Journal*, 96(2), 391-397.

Benmouiza, K., & Cheknane, A. (2013). Forecasting hourly global solar radiation using hybrid k-means and nonlinear autoregressive neural network models. *Energy Conversion and Management*, *75*, 561-569.

Bodri, B. (2001). A neural-network model for earthquake occurrence. *Journal of Geodynamics*, 32(3), 289-310.

Cao, J., & Lin, X. (2008). Study of hourly and daily solar irradiation forecast using diagonal recurrent wavelet neural networks. *Energy Conversion and Management*, *49*(6), 1396-1406.

Cheng, E. S., Chen, S., &Mulgrew, B. (1996). Gradient radial basis function networks for nonlinear and nonstationary time series prediction. *Neural Networks, IEEE Transactions on*, 7(1), 190-194.

Connor, J. T., Martin, R. D., & Atlas, L. E. (1994). Recurrent neural networks and robust time series prediction. *Neural Networks, IEEE Transactions on*, 5(2), 240-254.

Elizondo, D., Hoogenboom, G., & McClendon, R. W. (1994). Development of a neural network model to predict daily solar radiation. *Agricultural and Forest Meteorology*, 71(1), 115-132.

Fidan, M., Hocaoğlu, F. O., & Gerek, Ö. N. (2014). Harmonic analysis based hourly solar radiation forecasting model. *IET Renewable Power Generation*, *9*(3), 218-227.

Frank, E., Mayo, M., & Kramer, S. (2015). Alternating Model Trees. *In Proceedings of the 30th Annual ACM Symposium on Applied Computing*, 871-878.

Geiger, M., Diabaté, L., Ménard, L., & Wald, L. (2002). A web service for controlling the quality of measurements of global solar irradiation. *Solar energy*, 73(6), 475-480.

Geman, Stuart; E. Bienenstock; R. Doursat (1992). Neural networks and the bias/variance dilemma. *Neural Computation*, 4: 1–58.

Giles, C. L., Lawrence, S., & Tsoi, A. C. (2001). Noisy time series prediction using recurrent neural networks and grammatical inference. *Machine learning*, 44(1-2), 161-183.

Grant, R. H., Hollinger, S. E., Hubbard, K. G., Hoogenboom, G., &Vanderlip, R. L. (2004). Ability to predict daily solar radiation values from interpolated climate records for use in crop simulation models. *Agricultural and forest meteorology*, 127(1), 65-75.

Gueymard, C. A. (2003). Direct solar transmittance and irradiance predictions with broadband models. Part I: detailed theoretical performance assessment. *Solar Energy*, 74(5), 355-379.

Hamilton, C., Potter, W. , Hoogenboom, G. , McClendon, R., & Hobbs, W. (2015). Solar Radiation Time Series Prediction. *International Journal of Computer, Control, Quantum and Information Engineering*, 9(5), 656 - 661.

Heaton, J. (2011). *Introduction to the Math of Neural Networks.* Heaton Research, Inc.

Ho, S. L., Xie, M., & Goh, T. N. (2002). A comparative study of neural network and Box-Jenkins ARIMA modeling in time series prediction. *Computers & Industrial Engineering*, 42(2), 371-375.

Hocaoğlu, F. O., Gerek, Ö. N., & Kurban, M. (2008). Hourly solar radiation forecasting using optimal coefficient 2-D linear filters and feed-forward neural networks. *Solar Energy*, *82*(8), 714-726.

Hoerl, A. E., & Kennard, R. W. (1970). Ridge regression: Biased estimation for nonorthogonal problems. *Technometrics*, 12(1), 55-67.

Hoff, T. E., Perez, R., Kleissl, J., Renne, D., & Stein, J. (2013). Reporting of irradiance modeling relative prediction errors. *Progress in Photovoltaics: Research and Applications*, 21(7), 1514-1519.

Hoogenboom, G., Jones, J. W., Wilkens, P. W., Batchelor, W. D., Bowen, W. T., Hunt, L. A., ... & White, J. W. (1994). Crop models. *DSSAT version*, 3(2), 95-244.

Hornik, K., Stinchcombe, M., & White, H. (1989). Multilayer feedforward networks are universal approximators. *Neural networks*, 2(5), 359-366.

Horrigan L, Lawrence RS, Walker P (2002) How sustainable agriculture can address the environmental and human health harms of industrial agriculture. *Environmental Health Perspectives* 110: 445–456.

Huang, J., Korolkiewicz, M., Agrawal, M., & Boland, J. (2013). Forecasting solar radiation on an hourly time scale using a Coupled AutoRegressive and Dynamical System (CARDS) model. *Solar Energy, 87*, 136-149.

Igel, C. & Hüsken, M. (2000) Improving the Rprop Learning Algorithm. *Second International Symposium on Neural Computation* (NC 2000), 115-121.

Igel,C. & Hüsken, M. (2003) Empirical Evaluation of the Improved Rprop Learning Algorithm. *Neurocomputing* 50:105-123.

Intergovernmental Panel on Climate Change. (2015). *Climate Change 2014: Impacts, Adaptation, and Vulnerability.* Geneva, Switzerland.

Izgi, E., Öztopal, A., Yerli, B., Kaymak, M. K., & Şahin, A. D. (2012). Short–mid-term solar power prediction by using artificial neural networks. *Solar Energy, 86*(2), 725-733.

Jensen, A., & la Cour-Harbo, A. (2001). *Ripples in mathematics: the discrete wavelet transform*. Springer.

Ji, W., & Chee, K. C. (2011). Prediction of hourly solar radiation using a novel hybrid model of ARMA and TDNN. *Solar Energy, 85*(5), 808-817.

Khashei, M., & Bijari, M. (2011). A novel hybridization of artificial neural networks and ARIMA models for time series forecasting. *Applied Soft Computing*, 11(2), 2664-2675.

Kim, K. J. (2003). Financial time series forecasting using support vector machines. *Neurocomputing*, 55(1), 307-319.

Levenberg, K. (1944). A method for the solution of certain non–linear problems in least squares. *Quarterly of Applied Mathematics*, 2, 164-168.

Li, B., McClendon, R. W., & Hoogenboom, G. (2004). Spatial interpolation of weather variables for single locations using artificial neural networks. *Transactions of the ASAE*, 47(2), 629-637.

Marquardt, D. W. (1963). An algorithm for least-squares estimation of nonlinear parameters. *Journal of the Society for Industrial & Applied Mathematics*, *11*(2), 431-441.

Marquez, R., & Coimbra, C. F. (2011). Forecasting of global and direct solar irradiance using stochastic learning methods, ground experiments and the NWS database. *Solar Energy*, *85*(5), 746-756.

Mellit, A., Menghanem, M., & Bendekhis, M. (2005, June). Artificial neural network model for prediction solar radiation data: application for sizing stand-alone photovoltaic power system. In *Power Engineering Society General Meeting, 2005. IEEE* (pp. 40-44). IEEE.

Mellit, A., & Pavan, A. M. (2010). A 24-h forecast of solar irradiance using artificial neural network: Application for performance prediction of a grid-connected PV plant at Trieste, Italy. *Solar Energy*, 84(5), 807-821.

Ömer-Faruk, D. (2010). A hybrid neural network and ARIMA model for water quality time series prediction. *Engineering Applications of Artificial Intelligence*, 23(4), 586-594.

Paoli, C., Voyant, C., Muselli, M., & Nivet, M. L. (2010). Forecasting of preprocessed daily solar radiation time series using neural networks. *Solar Energy*, 84(12), 2146-2160.

Pedro, H. T., & Coimbra, C. F. (2012). Assessment of forecasting techniques for solar power production with no exogenous inputs. *Solar Energy*, *86*(7), 2017-2028.

Perez, R., Kivalov, S., Schlemmer, J., Hemker, K., Renné, D., & Hoff, T. E. (2010). Validation of short and medium term operational solar radiation forecasts in the US. *Solar Energy*, *84*(12), 2161-2172.

Rehman, S., & Mohandes, M. (2008). Artificial neural network estimation of global solar radiation using air temperature and relative humidity. *Energy Policy*, 36(2), 571-576.

Reikard, G. (2009). Predicting solar radiation at high resolutions: A comparison of time series forecasts. *Solar Energy, 83*(3), 342-349.

Richardson, C.W. & Wright, D.A. (1984). WGEN: A model for generating daily weather variables. U.S. Department of Agriculture, Agricultural Research Service, *ARS-8*, 83.

Riedmiller, M. (1994). *Rprop-Description and Implementation Details: Technical Report*. Inst. f. Logik, Komplexität u. Deduktionssysteme.

Rigollier, C., Bauer, O., & Wald, L. (2000). On the clear sky model of the ESRA—European Solar Radiation Atlas—with respect to the Heliosat method. *Solar energy*, 68(1), 33-48.

Ripley, B. (1996). *Pattern recognition and neural networks*. Cambridge University Press.

Sammut, C., & Webb, G. I. (Eds.). (2011). Bias–Variance Decomposition. In *Encyclopedia of machine learning* (pp. 100-101.). Springer Science & Business Media.

Sfetsos, A., & Coonick, A. H. (2000). Univariate and multivariate forecasting of hourly solar radiation with artificial intelligence techniques. *Solar Energy*,*68*(2), 169-178.

Southern Company. (2016). Renewable Resources. Retrieved April 08, 2016, from http://www.southerncompany.com/what-doing/corporate-responsibility/energy-innovation/building-renewable-resources.cshtml#solar

Spokas, K., & Forcella, F. (2006). Estimating hourly incoming solar radiation from limited meteorological data. *Weed science*, 54(1), 182-189.

Thissen, U., Van Brakel, R., De Weijer, A. P., Melssen, W. J., &Buydens, L. M. C. (2003). Using support vector machines for time series prediction. *Chemometrics and intelligent laboratory systems*, 69(1), 35-49.

Thornton, P. E., Hasenauer, H., & White, M. A. (2000). Simultaneous estimation of daily solar radiation and humidity from observed temperature and precipitation: an application over complex terrain in Austria. *Agricultural and Forest Meteorology*, 104(4), 255-271.

UGA Office of Sustainability. (2016). Renewable Energy. Retrieved April 08, 2016, from http://sustainability.uga.edu/what-were-doing/renewable-energy/

UGA Office of Sustainability. (2016). Solar power initiatives expand across campus. Retrieved April 08, 2016, from http://sustainability.uga.edu/solar-power-initiatives-expand-across-campus/

Wang, F., Mi, Z., Su, S., & Zhao, H. (2012). Short-term solar irradiance forecasting model based on artificial neural network using statistical feature parameters. *Energies*, *5*(5), 1355-1370.

Witten, I., Frank, E., & Hall, M. (2011). *Data Mining: Practical Machine Learning Tools and Techniques*. Los Altos, USA: Morgan Kaufmann.

Wong, L. T., & Chow, W. K. (2001). Solar radiation model. *Applied Energy*, 69(3), 191-224.

World Population Prospects, the 2012 Revision. (2012). Retrieved April 5, 2015, from http://esa.un.org/wpp/

Yang, K., Huang, G. W., & Tamai, N. (2001). A hybrid model for estimating global solar radiation. *Solar energy*, 70(1), 13-22.

Zhang, G. P. (2003). Time series forecasting using a hybrid ARIMA and neural network model. *Neurocomputing*, 50, 159-175.